Spontaneous Anomalous and Spin Hall Effects Due to Spin-Orbit Scattering of Evanescent Wave Functions in Magnetic Tunnel Junctions

A. Vedyayev,[1,2,*] N. Ryzhanova,[1,2] N. Strelkov,[1,2] and B. Dieny[2,†]

[1]*Department of Physics, Moscow Lomonosov State University, Moscow 119991, Russia*

[2]*SPINTEC, UMR 8191 CEA-INAC/CNRS/UJF-Grenoble 1/Grenoble-INP, 38054 Grenoble, France*

(Received 19 September 2012; published 13 June 2013)

We theoretically investigated the anomalous Hall effect (AHE) and spin Hall effect (SHE) transversal to the insulating spacer I, in magnetic tunnel junctions of the form F/I/F where the F's are ferromagnetic layers and I represents a tunnel barrier. We considered the case of purely ballistic (quantum mechanical) transport. These effects arise because of the asymmetric scattering of evanescent wave functions due to the spin-orbit interaction in the tunnel barrier. The AHE and SHE we investigated have a surface nature due to the proximity effect. Their amplitude is of first order in the scattering potential. This contrasts with ferromagnetic metals wherein these effects are of second (side-jump scattering) and third (skew scattering) order in these potentials. The value of the AHE current in the insulating spacer may be much larger than that in metallic ferromagnetic electrodes. For the antiparallel orientation of the magnetizations in the two F electrodes, a spontaneous Hall current exists even at zero applied voltage.

DOI: 10.1103/PhysRevLett.110.247204 PACS numbers: 85.75.−d, 71.70.Ej, 73.50.Jt, 75.76.+j

The anomalous Hall effect (AHE) in ferromagnetic metals and spin Hall effect (SHE) in nonmagnetic materials have attracted renewed interest in recent years. AHE and SHE have the same origin, namely spin-orbit interaction in the presence of magnetic ordering for AHE and without magnetic ordering for SHE. Detailed analyses of the mechanisms responsible for these two effects can be found in reviews [1–3]. These mechanisms are divided into two groups: intrinsic and extrinsic ones. The former appear in pure metals and have a topological nature, closely connected with Berry curvature. Extrinsic mechanisms are due to asymmetric electron scattering on defects in the presence of spin-orbit interaction. Two main types of scattering are considered: skew scattering [4,5] and side-jump scattering [6]. Most of theoretical papers on AHE and SHE considered the case of infinite homogeneous samples. References [7,8] also investigated AHE for multilayers and for highly inhomogeneous media.

Let's consider magnetic tunnel junctions, or MTJs (i.e., a sandwich of two ferromagnetic layers separated by a dielectric spacer) (Fig. 1) submitted to a bias voltage applied between the two F electrodes that are supposed to be made of the same ferromagnetic material. In this study, we are primarily interested in the Hall voltage which may appear between the opposite sides of the tunnel barrier due to the Hall current inside the spacer in the presence of spin-orbit scattering on the impurities. We will show that these Hall and spin Hall currents do exist and that moreover, for the antiparallel orientation of the magnetizations in the two ferromagnetic layers, a spontaneous transverse Hall current exists, even in the absence of any applied bias voltage.

The Hall currents were calculated using Keldysh formalism [9]. The electrons were described as forming a free electron gas submitted to an s-d exchange interaction. As an example, the Green functions for the considered system (Fig. 1) and for z projection of the electron's spin antiparallel to the magnetization in the left electrode are:

$$G^{\uparrow}_{\mathrm{AP},x>x'}(r,r') = \frac{1}{N}\sum_{\varkappa} -\frac{1}{2q\mathfrak{D}} e^{i\varkappa_i(y-y')} e^{i\varkappa_z(z-z')} \times (e^{q(x-x_2)}(q+ik_2) + e^{-q(x-x_2)}(q-ik_2)) \times (e^{q(x'-x_1)}(q-ik_1) + e^{-q(x'-x_2)}(q+ik_1)), \tag{1}$$

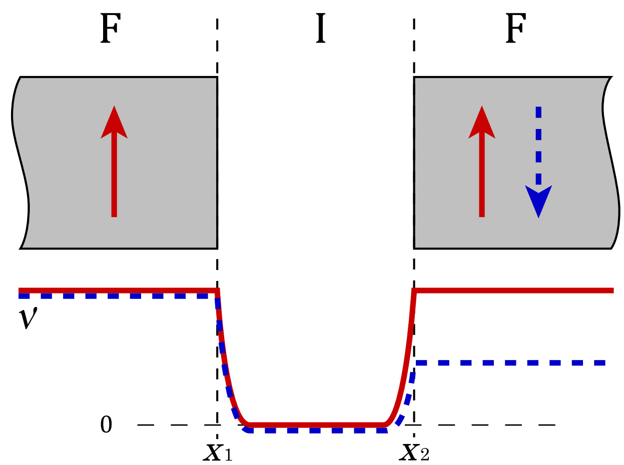

FIG. 1 (color online). Schematic illustration of a MTJ. The F's are the ferromagnetic layers, and I the insulating spacer. Arrows denote the direction of magnetizations in the electrodes, for parallel (P) and antiparallel (AP) orientations. The bottom curve schematically illustrates the dependence of density of states (ν is in arbitrary units) of spin up tunnelling electrons on the distance from the interface for P and AP orientations.

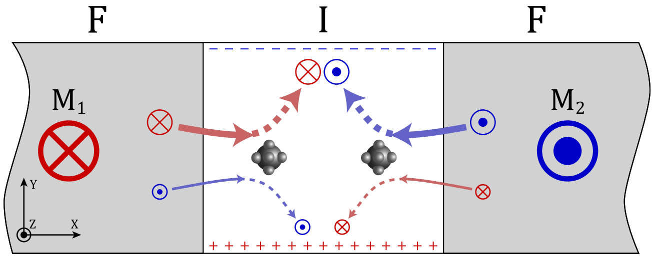

FIG. 2 (color online). Schematic illustration of the AHE and SHE in a MTJ due to spin-orbit scattering on impurities. ⊗ and ⊙ denote the direction of magnetizations and electron spins. The thickness of the lines are proportional to Hall currents for the given projection of spin.

$$G^{\uparrow}_{\mathrm{AP},x<x'}(r,r') = \frac{1}{N}\sum_{\varkappa} -\frac{1}{2q\mathfrak{D}} e^{i\varkappa_i(y-y')} e^{i\varkappa_z(z-z')}[e^{q(x-x_1)} \times (q-ik_1) + e^{-q(x-x_2)}(q+ik_1)] \times [e^{q(x'-x_2)}(q+ik_2) + e^{-q(x'-x_2)}(q-ik_2)], \quad (2)$$

where:

$$\mathfrak{D} = [e^{qb}(q-ik_1)(q-ik_2) - e^{-qb}(q+ik_1)(q+ik_2)],$$

$$q = \sqrt{\frac{2m}{\hbar^2}(U-E) + \varkappa^2},$$

$$k_{1,2} = \sqrt{\frac{2m}{\hbar^2}(E \pm J_{sd}) - \varkappa^2}. \quad (3)$$

In (1) and (2) "AP" denotes the antiparallel orientation of magnetizations in the two ferromagnetic electrodes and x_1 and x_2 are the ferromagnetic and insulator interface coordinates, respectively. In (3), U is the barrier height, E is the electron energy, J_{sd} is the s-d exchange energy. For the opposite direction of spin, all projection changes in (1) and (2) are straightforward. From (1) and (2), it follows that for the considered system, a finite density of states exists in the energy gap within the barrier due to the proximity effect, which decreases exponentially with the distance from F/I interfaces (Fig. 1). In other words, a quasi-two-dimensional electron gas exists inside the barrier near the interfaces. Similar to a three-dimensional topological insulator, this electron gas can give birth to charge and spin currents [10]. Evidently the mechanisms of creation of these surface states are different in the two cases. Let's suppose now that the tunnelling electrons experience scattering on impurities within the barrier with spin-orbit interaction. This asymmetric scattering deviates the electrons in the direction perpendicular to the tunnel current and to the projection of their spin. So if the current is spin-polarized, a Hall current appears transversally to the tunnel barrier. Quite interestingly, in an antiparallel magnetic configuration of the MTJ, this nondissipative current appears spontaneously even in the absence of bias voltage applied across the tunnel barrier (see Fig. 2).

This implies that if the MTJ is fabricated in the form of a closed ring, a persistent spontaneous Hall current would exist within the tunneling barrier in an AP magnetic configuration. Experimentally, such a system could be prepared for instance by depositing the MTJ stack by a physical vapor deposition (PVD) technique (i.e., sputtering) on a rotating cylinder, the magnetization of the MTJ magnetic electrodes being oriented "up" or "down" parallel to the cylinder axis, the two magnetic electrodes having a different switching field so as to be able to control the MTJ magnetic configuration (parallel or antiparallel).

To investigate this effect we added into the free electron Hamiltonian, the impurity potential including spin-orbit interaction and calculated the induced perturbation to the wave functions:

$$\psi = \psi_0(r) + \int G(r,r')V_{\mathrm{so}}(r')\psi_0(r')d^3r' = \psi_0(r) + \int \delta(r'-r_i)(a_0^5\lambda_0)d^3r' \times \left[G(r,r')i\sigma_z\left(\frac{\overleftarrow{\partial}}{\partial x'}\frac{\vec{\partial}}{\partial y'} - \frac{\overleftarrow{\partial}}{\partial y'}\frac{\vec{\partial}}{\partial x'}\right)\psi_0(r')\right]. \quad (4)$$

In (4) λ_0 represents the intensity of the spin-orbit interaction, a_0 the lattice parameter, r_i the position of the impurity, and σ_z the z component of the Pauli matrix. The zero-order wave function for the left-to-right and right-to-left tunnelling electrons are correspondently:

$$\psi^{\uparrow}_{\mathrm{AP},l} = \frac{2\sqrt{k_1}}{\mathfrak{D}} \times [e^{q(x-x_2)}(q+ik_2) + e^{-q(x-x_2)}(q-ik_2)], \quad (5)$$

$$\psi^{\uparrow}_{\mathrm{AP},r} = \frac{2\sqrt{k_2}}{\mathfrak{D}} \times [e^{q(x-x_1)}(q-ik_1) + e^{-q(x-x_1)}(q+ik_1)]. \quad (6)$$

Now it is easy to calculate the Hall current in the ballistic regime of the first order in the spin-orbit interaction:

$$j_H^{\sigma} = \frac{e}{2\pi\hbar}\int\frac{f(E)}{(2\pi)^2}dE \times \int i\sigma_z\left(\psi_l^{\sigma}\frac{\partial}{\partial y}\psi_l^{\sigma *} - \psi_l^{\sigma *}\frac{\partial}{\partial y}\psi_l^{\sigma}\right)^{(1)}d\varkappa_y d\varkappa_z + \frac{e}{2\pi\hbar}\int\frac{f(E+eV)}{(2\pi)^2}dE \times \int i\sigma_z\left(\psi_r^{\sigma}\frac{\partial}{\partial y}\psi_r^{\sigma *} - \psi_r^{\sigma *}\frac{\partial}{\partial y}\psi_r^{\sigma}\right)^{(1)}d\varkappa_y d\varkappa_z, \quad (7)$$

where $f(E)$ is the Fermi distribution for the left electrode, $f(E+eV)$ the same for the right one, and V the applied voltage. The superscript "(1)" denotes the first order terms in the spin-orbit interaction in the expression in large parentheses.

Substituting (4)–(6), into (7) and averaging on the position of impurities r_i yield the following expressions for the spin-up Hall current originating respectively from left (l) and right (r) electrodes in AP configuration:

$$
\begin{aligned}
j^{\uparrow}_{\mathrm{AP},l} \sim \int d\varkappa_y d\varkappa_z dE \frac{4\lambda_0 \varkappa_y^2 k_1}{|\mathfrak{D}|^4} f(E) \\
&\times \{(e^{2q(x-x_2)}e^{-2qb} - e^{-2q(x-x_2)}e^{2qb})(q^2+k_2^2)^2 \\
&+ 2(e^{2qb}-e^{-2qb})(q^2-k_2^2)(k_1^2-k_2^2) \\
&+ (e^{2q(x-x_1)} - e^{-2q(x-x_1)})(q^2+k_2^2)[(q^2+k_1^2) \\
&+ (k_1^2-k_2^2)] - 2(e^{2q(x-x_2)} - e^{-2q(x-x_2)}) \\
&\times [(q^2-k_1k_2)^2 - q^2(k_1+k_2)^2]\}, \qquad (8)
\end{aligned}
$$

$$
\begin{aligned}
j^{\uparrow}_{\mathrm{AP},r} \sim \int d\varkappa_y d\varkappa_z dE \frac{4\lambda_0 \varkappa_y^2 k_2}{|\mathfrak{D}|^4} f(E+eV)\{(e^{2q(x-x_1)}e^{2qb} \\
&- e^{-2q(x-x_1)}e^{-2qb})(q^2+k_1^2)^2 + 2(e^{2qb}-e^{-2qb}) \\
&\times (q^2-k_1^2)(k_1^2-k_2^2) + (e^{2q(x-x_2)} - e^{-2q(x-x_2)}) \\
&\times (q^2+k_1^2)[(q^2+k_2^2) - (k_1^2-k_2^2)] \\
&- 2(e^{2q(x-x_1)} - e^{-2q(x-x_1)})[(q^2-k_1k_2)^2 \\
&- q^2(k_1+k_2)^2]\}. \qquad (9)
\end{aligned}
$$

For the sake of simplicity, we wrote these expressions for the case of a rectangular barrier, but in the final expressions, we took into account the trapezoidal deformation of the barrier resulting from the application of a bias voltage.

From (8) and (9), it follows that the Hall current exponentially depends on the coordinate x and reaches its maximum near the "left" interface for the "left" electrons and at the "right" interface for "right" electrons. This emphasizes the surface nature of the considered Hall effect.

It's interesting to note that the present Hall effect in the MTJ barrier appears at first order on the scattering potential, whereas for infinite ferromagnetic metals the Hall effect is in third order on the scattering potential for skew scattering and in second order for the side-jump mechanism [1–3]. This difference is due to the strong inhomogeneity of the considered system in x direction. The other remarkable difference already pointed out is that this Hall effect spontaneously exists even at zero bias voltage in MTJs.

Next the obtained expressions for Hall currents and spin Hall currents were averaged over the coordinate x and integration over momentum $\vec{\varkappa}$ and energy E yields in the limit $e^{-2qb} \ll 1$, in the parallel configuration of the MTJ:

$$
\langle j^{\uparrow+\downarrow}_{l+r}\rangle^{\mathrm{P,skew}}_{\mathrm{AHE}} = \frac{4}{15\pi}\frac{e^2}{2\pi\hbar}\frac{\tilde{\lambda}c}{U^2 b}\left(E_F^{\uparrow 2}\frac{k_F^{\uparrow 3}}{q_0^2} - E_F^{\downarrow 2}\frac{k_F^{\downarrow 3}}{q_0^2}\right)\frac{V}{2q_0 b},
$$

$$
\langle j^{\uparrow+\downarrow}_{l+r}\rangle^{\mathrm{P,skew}}_{\mathrm{SHE}} = \frac{4}{15\pi}\frac{e^2}{2\pi\hbar}\frac{\tilde{\lambda}c}{U^2 b}\left(E_F^{\uparrow 2}\frac{k_F^{\uparrow 3}}{q_0^2} + E_F^{\downarrow 2}\frac{k_F^{\downarrow 3}}{q_0^2}\right)\frac{V}{2q_0 b},
$$

and in the antiparallel configuration:

$$
\langle j^{\uparrow+\downarrow}_{l+r}\rangle^{\mathrm{AP,skew}}_{\mathrm{AHE}} = \frac{16}{105\pi}\frac{e}{2\pi\hbar}\frac{\tilde{\lambda}c}{U^2 b}(E_F^{\uparrow 3}k_F^{\uparrow} - E_F^{\downarrow 3}k_F^{\downarrow} + O(V^2)),
$$

$$
\langle j^{\uparrow+\downarrow}_{l+r}\rangle^{\mathrm{AP,skew}}_{\mathrm{SHE}} = \langle j^{\uparrow+\downarrow}_{l+r}\rangle^{\mathrm{P,skew}}_{\mathrm{SHE}},
$$

where $\tilde{\lambda} = 2ma_0^2\lambda_0/\hbar^2$ is the dimensionless constant of the spin-orbit interaction, c the atomic concentration of impurities, and $q_0 = \sqrt{2m(U-E)/\hbar}$.

One may notice that in contrast to the tunnelling current through the tunnel barrier, the expressions of the Hall and spin Hall currents do not contain the small parameter e^{-2qb}. Instead, the averaged Hall voltage decreases inversely proportional to the barrier thickness. Its amplitude is proportional to the small parameter λ_0 related to the intensity of the spin-orbit interaction. The absence of e^{-2qb} in the expression for j_H further indicates that these predicted Hall and spin Hall effects have a surface nature in contrast to the tunnelling current.

Up to now, the case of "skew" scattering has been considered. In addition to this scattering mechanism, another contribution to Hall and spin Hall currents originates from another term in the operator of quantum mechanical velocity, proportional to the spin-orbit interaction:

$$
\hat{v} = \frac{d}{dt}\vec{r} = -i[\vec{r}\times\vec{H}] = \frac{\hbar\vec{k}}{m} + \lambda[\vec{\sigma}\times\vec{\nabla}V(\vec{r})], \qquad (10)
$$

where $V(\vec{r})$ is the potential of impurity and λ the spin-orbit constant. This additional contribution to the Hall current is equivalent to a "side-jump" mechanism [1]. In the present case it is written in final form as:

$$
\langle j^{\uparrow+\downarrow}_{l+r}\rangle^{\mathrm{P,sj}}_{\mathrm{AHE}} = \frac{4}{15\pi}\frac{e^2}{2\pi\hbar}\frac{\tilde{\lambda}c}{U^2 b}\left(E_F^{\uparrow 2}\frac{k_F^{\uparrow 3}}{q_0^2} - E_F^{\downarrow 2}\frac{k_F^{\downarrow 3}}{q_0^2}\right)\frac{V}{2q_0 b},
$$

$$
\langle j^{\uparrow+\downarrow}_{l+r}\rangle^{\mathrm{P,sj}}_{\mathrm{SHE}} = \frac{4}{15\pi}\frac{e^2}{2\pi\hbar}\frac{\tilde{\lambda}c}{U^2 b}\left(E_F^{\uparrow 2}\frac{k_F^{\uparrow 3}}{q_0^2} + E_F^{\downarrow 2}\frac{k_F^{\downarrow 3}}{q_0^2}\right)\frac{V}{2q_0 b},
$$

$$
\langle j^{\uparrow+\downarrow}_{l+r}\rangle^{\mathrm{AP,sj}}_{\mathrm{AHE}} = \frac{8}{15\pi}\frac{e}{2\pi\hbar}\frac{\tilde{\lambda}c}{Ub}\times(E_F^{\uparrow 2}k_F^{\uparrow} - E_F^{\downarrow 2}k_F^{\downarrow}O(V^2)),
$$

$$
\langle j^{\uparrow+\downarrow}_{l+r}\rangle^{\mathrm{AP,sj}}_{\mathrm{SHE}} = \langle j^{\uparrow+\downarrow}_{l+r}\rangle^{\mathrm{P,sj}}_{\mathrm{SHE}}.
$$

First, we note that both contributions to the Hall and spin Hall currents are proportional to the concentration of impurities. This is in contrast to the usual Hall conductivity in ferromagnetic metals which is inversely proportional to this concentration for the skew scattering and does not depend on the concentration for the side-jump mechanism. However in the present case, the Hall current in metallic ferromagnetic electrodes is proportional to the drop in voltage in this electrode, itself proportional to the small parameter e^{-2qb}. Therefore, for a thick enough insulating spacer, Hall and spin Hall effects inside the spacer may become much larger than the corresponding effects within the ferromagnetic electrodes.

To estimate the Hall voltage V_H, the expressions of the Hall current linear on the applied voltage have to be divided by the conductance in the y direction:

$$G = \frac{e^2}{2\pi\hbar}\frac{1}{b}\sqrt{\frac{2m}{\hbar^2}U} \times \left[\left(1 - \sqrt{1 - \frac{E_F^{\uparrow}}{U}}\right) + \left(1 - \sqrt{1 - \frac{E_F^{\downarrow}}{U}}\right)\right]. \quad (11)$$

Estimated values of V_H are in the range 10^{-6} to 10^{-4} V, for $\tilde{\lambda}$ in the interval 10^{-2} to 10^{-1} and c in the interval 0.01 to 0.1. These range of values of $\tilde{\lambda}$ correspond to the limits between typical $3d$ metals in which the spin-orbit constant is of the order of 0.02 eV [11] and the case of Pt in FePt alloys for which the spin orbit constant is 0.54 eV [12]. In our calculation, these values are normalized by the characteristic energy $\hbar^2/2ma^2$ ($\hbar$ is Planck's constant, m the electron mass, and a the atomic spacing) of 3.4 eV. To experimentally measure this new type of AHE due to spin-orbit scattering of evanescent wave function it is necessary to fabricate the MTJ with the dielectric spacer (Al_2O_3, MgO) doped by ions of heavier metals (for instance Zn as in MgZnO based MTJ [13]) or even use heavy metal oxides with large spin-orbit interaction, for example TbO_x, TaO_x [14] or HfO_x [15]. Furthermore, since this predicted spontaneous AHE in AP configuration does not carry any energy, its measurement is not straightforward. One possibility is to detect it during the magnetization switching of the MTJ magnetic electrodes. This would be similar to the readout technique used in ferroelectric memories. There, the information stored in the form of an electrical dipole orientation in a ferroelectric element is detected by switching the electrical dipole orientation and detecting the charge flow associated with this dipole switching. This charge flow is integrated by a capacity yielding a final output voltage proportional to the integrated amount of charge displaced during the dipole switching. In MTJs a similar charge flow due to the variation in the AHE could be detected associated with magnetization switching by connecting a capacity between the electrical contacts transverse to the tunnel junction. Finally, we have to notice that due to the redistribution of charge and potential near the interfaces inside the barrier, an additional Rashba term in the spin-orbit interaction may appear [16]. But at the atomic scale, this effect renormalizes the atomic potential of the impurities near the interfaces, so it may be taken into account by renormalization of the spin-orbit constant $\tilde{\lambda}$.

This work was partly funded by the European Commission through the ERC HYMAGINE Grant No. ERC 246942 and Russian Fund of Basic Research Grant No. 130201452A.

*vedy@magn.ru
†bernard.dieny@cea.fr

[1] P. Wölfle and K. A. Muttalib, Ann. Phys. (Amsterdam) **15**, 508 (2006).
[2] N. Nagaosa, J. Phys. Soc. Jpn. **75**, 042001 (2006).
[3] N. Nagaosa, J. Sinova, S. Onoda, A. H. MacDonald, and N. P. Ong, Rev. Mod. Phys. **82**, 1539 (2010).
[4] J. Smit, Physica (Amsterdam) **21**, 877 (1955).
[5] J. Smit, Phys. Rev. B: Solid State **8**, 2349 (1973).
[6] L. Berger, Phys. Rev. B: Solid State **2**, 4559 (1970).
[7] N. Ryzhanova, A. Vedyayev, A. Crépieux, and C. Lacroix, Phys. Rev. B **57**, 2943 (1998).
[8] A. Granovsky, A. Vedyayev, and F. Brouers, J. Magn. Magn. Mater. **136**, 229 (1994).
[9] L. V. Keldysh, Sov. Phys. JETP **20**, 1018 (1965).
[10] M. Z. Hasan and C. L. Kane, Rev. Mod. Phys. **82**, 3045 (2010).
[11] A. Fert and O. Jaoul, Phys. Rev. Lett. **28**, 303 (1972).
[12] H. Zhang, F. Freimuth, S. Blugel, Y. Mokrousov, and I. Souza, Phys. Rev. Lett. **106**, 117202 (2011).
[13] S. S. P. Parkin, US Patent No. 7606010 (2007).
[14] L. S. Dorneles, R. L. Sommer, and L. F. Schelp, J. Appl. Phys. **91**, 7971 (2002).
[15] C. L. Platt, B. Dieny, and A. E. Berkowitz, Appl. Phys. Lett. **69**, 2291 (1996).
[16] L. Xu and S. Zhang, J. Appl. Phys. **111**, 07C501 (2012).